NJC

Accepted Manuscript

This is an *Accepted Manuscript*, which has been through the Royal Society of Chemistry peer review process and has been accepted for publication.

Accepted Manuscripts are published online shortly after acceptance, before technical editing, formatting and proof reading. Using this free service, authors can make their results available to the community, in citable form, before we publish the edited article. We will replace this *Accepted Manuscript* with the edited and formatted *Advance Article* as soon as it is available.

You can find more information about *Accepted Manuscripts* in the **Information for Authors**.

Graphical abstract
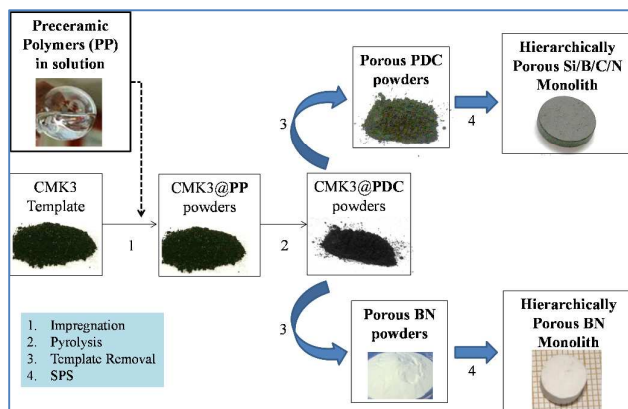
Sentence for TOC

This review describes the elaboration of ordered mesoporous non oxide materials such as BN and SiBCN and the subsequent fabrication of derived monoliths by Spark Plasma Sintering using the as-prepared powders

Journal Name

ARTICLE

Ordered Mesoporous Polymer-Derived Ceramics and their Processing into Hierarchically Porous Boron Nitride and SilicoBoron CarboNitride Monoliths

Samuel BERNARD and Philippe MIELE*

Inorganic porous materials are widely used in a number of applications, where there is a need to produce materials with a controlled and/or multiscale porosity. In this category, periodic mesoporous boron- and silicon-based non-oxide ceramics frameworks with *p6mm* hexagonal symmetry attract increasing interest due to their plenty of unique properties, functionalities and potential applications. These materials are prepared by a hard-templating route (=nanocasting) of ordered mesoporous templates including silica (SBA-15) and carbon (CMK-3). In the first part of this perspective, the synthesis approach of ordered mesoporous boron nitride (BN) and silicoboron carbonitride (Si/B/C/N) is emphatically described including precursor selection and synthesis, nanocasting process, pyrolysis and template removal. In order to satisfy the requirement for practical applications, the second part of this perspective describes how a convenient powder processing approach that adopts the flexibility of powder-based processes (spark plasma sintering (SPS)) has been employed to produce without the use of any sintering additives mechanically stable, hierarchically porous BN and Si/B/C/N monoliths from ordered mesoporous powders.

A Introduction

The technological progress continuously calls for better advanced materials with optimized and new properties. Advanced materials span the whole *organic* → *inorganic* spectrum: 90% are polymeric and the remaining 10% are inorganic. Inorganic materials generally exhibit high chemical, mechanical, structural and thermal stabilities to be used in thermostructural applications. In this category, ceramics represent the materials of choice to operate in severe conditions such as in harsh environments (basic, acidic) and at high temperatures (~ 900 °C). The main family of ceramics having a great extent of physical and chemical properties, which are extensively used today is oxide. Therefore, the majority of studies in materials chemistry and physics are focused on such materials which are nowadays the best characterized group of inorganic compounds. However, they do not always cover the current technological needs, especially as porous candidates according to their limited thermostructural and thermochemical stabilities. Accordingly, there are growing efforts to find new oxygen-free compounds satisfying these technological requirements for porous materials. The most promising candidates for that are carbides, nitrides and carbonitrides.

In oxygen-free nitride ceramics, the nitrogen atom is combined with an element of similar or lower electronegativity such as boron, silicon and most metals. Nitrides contain the nitride ion N^{3-} and we can distinguish two categories of nitrides: the ionic-covalent family of nitrides and the transition metal series of the periodic table. In the category of covalently-bonded nitrides, the interest for hexagonal-boron nitride (*h*-BN but expressed here as BN) grew during the past decades in relation with its unique combination of key properties. BN is a

synthetic material, which was discovered in the early 19th century and developed as a commercial material at the latter half of the 20th century.[1] BN is similar in structure to graphite and consists of a honeycomb structure of boron and nitrogen atoms linked by sp[2] hybridized orbits and held together mainly by Van der Waals force. In comparison to graphite, the layered BN hexagons are arranged vertically and each nitrogen is surrounded by 2 boron atoms of the adjacent layers.[2] The polar nature of the B-N bond in sp[2]-bonded BN makes it a wide band gap insulator with different chemistry on its surface and exciting physical and chemical properties including, high thermal conductivity, high temperature stability and high resistance to corrosion and oxidation and strong UV emission.[3-7] It is chemically inert, nontoxic and it has good environmental compatibility.[1] BN also has enhanced physisorption properties due to the dipolar fields near its surface.[8] As porous, BN exhibit unique physical and chemical properties for applications in various fields especially those related to adsorption like gaseous uptake, pollutant adsorption and catalyst supports as well as those related to DNA translocation.[9-14]

Beside nitrides, oxygen-free carbonitride ceramics represent a large family of materials combining carbon and nitrogen elements. There are two categories of carbonitrides: on the one hand those with C-N bonds such as the nominal composition C_3N_4[15] and in the other hand the systems combining distinct nitride and carbide phases and free carbon such as the Si/C/N and Si/B/C/N systems.[16-17] The latter exhibit atomically homogenous elemental distributions and their main interest is the stability of their amorphous network at very high temperature. As an illustration, carbonitride ceramics based on the quaternary system Si/B/C/N are highly durable and display properties targeted for thermostructural applications.[18-30]

The fabrication of nitrides and carbonitrides is usually made by conventional powder technology requiring nitridation or carbothermal reaction of oxide compounds and use of additives during the further sintering process. Beside the fact that the use of oxide inherently induces the presence of oxygen-containing phases, the possibility to envisage nitrides and carbonitrides with shape, composition and texture complexities of the part which can be manufactured, especially those that display hierarchical porosity, *e.g.* micro and/or mesopores interconnected with a continuous macropores network, is rather limited. Within this context, a "ceramic through chemistry" concept has to be applied.[31-32]

The *Polymer-Derived Ceramics* (PDCs) route offers features that can extend the composition, texture complexity and therefore application of non-oxide ceramics.[16-17,33-44] It is indeed particularly adapted to the preparation of porous materials through the so-called nanocasting, *i.e.*, hard-template, methodology.[18,20,45-59] The so-called nanocasting provides access to tunable pore morphologies and allows to elaborate architectured PDCs by (*i*) replicating the nanostructure/architecture of a template material into a locally ordered pore system through the impregnation of the template with a preceramic polymer solution or melt, (*ii*) performing the subsequent pyrolysis then (*iii*) removing the mold. The

combination of the PDCs route and the nanocasting process is usually focused on the production of micrometer-sized powders with ordered mesoporosity. Mesoporous materials are interesting because their pore size is similar to the dimensions of many molecules, which suggests that these materials could be potentially useful in separation and catalytic processes. However, mesoporous powders have some difficulties in practical use and as a consequence a limited application. Practical applications require that the porous material is available in macroscopic form such as monolith.

The current technology for producing porous non-oxide ceramic monoliths involves extrusion or pressing powders together with sacrificial and sintering additives into an engineering shape, removal of all sacrificial additives and finally sintering at high temperature. Sintering additives are usually added to impart high mechanical strength. As an alternative, it would be interesting to combine the elaboration of ordered mesoporous powders with an approach that adopts the convenience and flexibility of powder-based processes such as spark plasma sintering (SPS) (Figure 1).
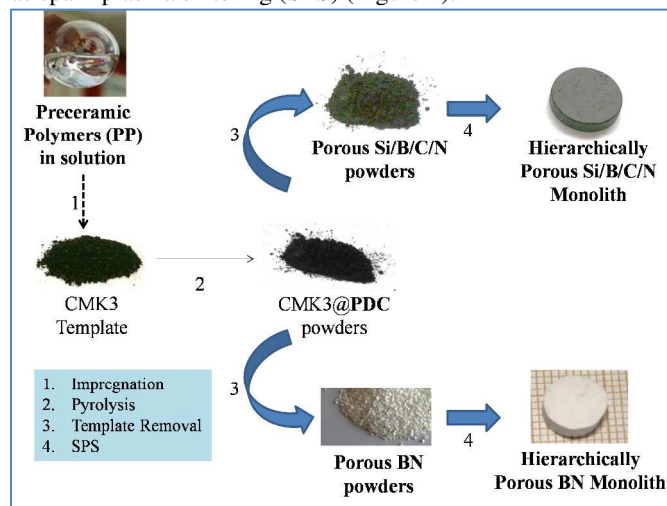
Figure 1. Overall synthetic path employed to generate hierarchically porous PDC monoliths coupling the PDCs route with nanocasting and SPS processes.

Herein, we review the preparation and characterization of **O**rdered **M**eso**P**orous BN and Si/B/C/N ceramics (labeled **OMP***X* with X being the considered system (BN or Si/B/C/N)) and their processing to prepare **H**ierarchically **P**orous BN and Si/B/C/N monoliths (labeled **HPM***X*) through SPS of the ordered mesoporous powders without the use of any sintering additives. These materials can represent potential candidates for integration into a device set-up where they could find applications as robust supports or host materials.

B Synthesis of ordered mesoporous BN and Si/B/C/N powders

Requested characteristics for the preparation of the polymer-derived ordered mesoporous ceramics are the following:

(1) The precursors are highly soluble for processability.

(2) The thermal decomposition occurs with a relatively low weight loss avoiding depolymerization and volatilization of low-weight molecular species for controlling porosity.

(3) The final temperature of template removal should be optimized to generate stable materials without loss of porosity.

However, combining such properties in only one molecule remains an ambitious objective to reach.

A BN and Si/B/C/N precursors

BN precursors are usually of two types. We can distinguish borazine and their derived polyborazylene[60] and *B*-tri(methylamino)borazine and the derived poly[*B*-(methylamino)borazine]. In our group, poly[*B*-(methylamino)borazine] is an appropriate candidate to successfully prepare BN fibers and ordered mesoporous BN.[39,47,61] *B*-tri(methylamino)borazine is composed of a borazine ring capped by $N(H)CH_3$ groups bound to boron atoms. The exact structure of the derived polymer, *i.e.*, poly[*B*-(methylamino)borazine], is not known. Presuming quantitative methylamine condensation of *B*-tri(methylamino)borazine, a polymer structure as presented in Fig. 2 is expected. Fig. 2 shows that the chemical environment of nitrogen atoms is modified during the polymerization, while boron atoms remain in a BN_3 environment.
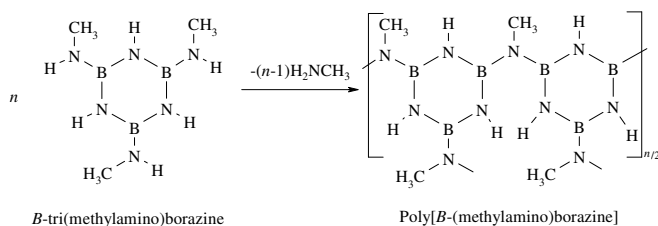
Figure 2. Methylamine condensation of *B*-tri(melthylamino)borazine yielding poly[*B*-(melthylamino)borazine].

Previous NMR investigations of Poly[*B*-(MethylAmino)Borazine] (PMAB, $[B_{3.0}N_{4.6}C_{2.1}H_{9.5}]_n)$[55b,f] showed that the buiding blocks of a typical poly[*B*-(methylamino)borazine] are composed of borazine rings, which are connected *via* a majority of NCH_3 bridges and a small amount of NB_3-containing motifs forming a cross-linked network. This branched molecular network is capped by a low proportion of peripheral $N(H)CH_3$ groups.

There are two main single-source molecular systems that lead to Si/B/C/N ceramics. The first synthetic pathway pioneered by Riedel *et al.* focuses on the synthesis of Boron-Modified PolySilazanes (BmPSs) of the type $[B(C_2H_4SiCH_3NH)_3]_n$ $(C_2H_4 = CH_3CH, CH_2CH_2)$.[21] They represent polysilazane rings which are cross-linked *via* -C-B-C-bridges (Fig. 3). The second approach proposed by Jansen *et al.* makes use of the synthesis of polyborosilazanes, *i.e.*, polysilazanes cross-linked *via* -B-N-B- bridges.[26]
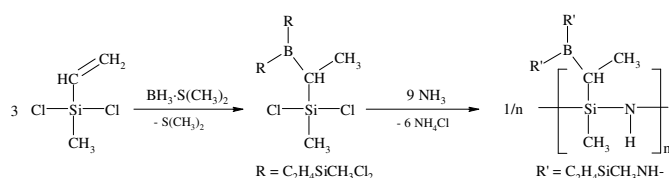
Figure 3. Synthesis procedure and idealized structures of BmPS of the type $[B(C_2H_4SiCH_3NH)_3]_n$ $(C_2H_4 = CH_3CH, CH_2CH_2)$.

In our own group, we have explored additional examples of BmPSs synthesis, and some progress has been made in understanding some of the stepwise chemistry that takes place in the formation and decomposition of single-source precursor systems. As an example, we re-investigated the synthesis of the BmPS of the type $[B(C_2H_4SiCH_3NH)_3]_n$ $(C_2H_4 = CH_3CH, CH_2CH_2)$ which was pioneered by Riedel *et al.* using lithium amide ($LiNH_2$) instead of ammonia as a network building agent with TrisDichloroSilylethylBorane (TDSB) (Fig. 4).[19] Further unpublished extensions on this system revealed that $LiNH_2$ allowed us to precisely controlled the quantity of $-NH_2$ groups introduced in the polymer building block of idealized composition ($[Si_3B_{1.1}C_{10.5}N_{3.0}H_{25.5}]_n$).
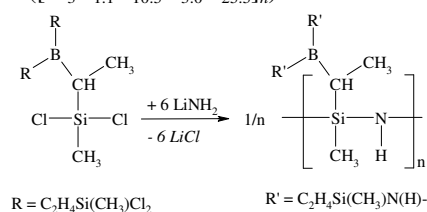
Figure 4. Reaction between TDSB and $LiNH_2$ leading to BmPSs of the type $[B(C_2H_4SiCH_3NH)_3]_n$ $(C_2H_4 = CH_3CH, CH_2CH_2)$.

The BmPS considered here is expected to be composed of cyclic silazane units $[-Si-N-]_n$ which are bridged by BC_3 units. Formally, every chlorine atom present in TDSB (6 atoms) is substituted by a NH_2 group. Subsequent condensation yields Si-N(H)-Si units. Ammonolysis with ammonia therefore requires at least 9 *eq.* of linking agent referred to TDSB. With $LiNH_2$ (Fig. 4), 6 *eq.* referred to TDSB are required.

Both tetrahedral and trigonal (distribution of BC_xN_{3-x} environments that can be assigned to BC_3, BCN_2 and BC_2N units) boron coordinations are present as it is usually observed for boron-modified polysilazanes.[62-64] The polymer displays silazane rings with $Si(CH_3)(NH)_2$, $Si-CH(B)-CH_3$ and $Si-CH_2-CH_2-B$ units confirming the lack of regio-selectivity of the borane dimethylsulfide according to the presence of both structural units, namely $CHCH_3$ and $-CH_2CH_2-$ bridges interconnecting Si and B in the native polymer.

B Synthesis of ordered mesoporous BN and Si/B/C/N powders

The use of carbon templates is generally preferred to confine preceramic polymers due to the pore surface chemistry of carbonaceous template that involves more complete pore filling, the expected better chemical compatibility of carbon with ceramic precursors and the opportunity to replicate the real

structure of silica. Mesoporous silica SBA-15 was prepared by hydrothermal synthesis then used as hard template to prepare mesoporous carbon CMK-3 by impregnation with sucrose according to established procedures.[65,66] CMK-3 exhibited a highly ordered 2-D hexagonal mesostructure with a specific surface area of 1052 m².g⁻¹ and pore diameters of 3.5 nm. The direct solution infiltration of CMK-3 with the previously described polymers at RT for 48 h under static vacuum is an effective method to fully infiltrate the pores of the template. The weight ratio of the polymer:template is optimized whereas an important step is the subsequent filtration step that consists to selectively remove the precursor molecules deposited outside while the capillary forces kept the precursor molecules effectively inside the pores. A further crucial part is the post-treatment of the infiltrated template at low pressure (5.10⁻² mbar at 40 °C) in order to slowly remove the solvent while generating a black powder. Lastly, the subsequent heat-treatments also are challenging because the ceramic yield has to be the highest possible to keep the maximum of products confined in the porosity of the template after the ceramic transformation and obtain after the template removal step a porous component with the expected ordered mesoporosity. It should be mentioned that the number of impregnation-pyrolysis cycles is optimized. However, as mentioned above, combining high solubility and high ceramic yield in a same polymer is complex. Indeed, a number of factors, such as the polymer structure, the molecular weight, the degree of cross-linking, *i.e.*, the structure of the polymer backbone and the nature of the functional groups that are attached to main polymer chain strongly, influence both properties.

Poly[*B*-(methylamino)borazine] exhibits an appreciable thermal stability up to ~150 °C in flowing nitrogen (Fig. 5a). The decomposition under nitrogen atmosphere occurs through two main steps from ~150 °C up to 450 °C and from 450 °C to 700 °C. The as-produced residue is obtained in *ca.* 58 % yield at 1000 °C and its black colour suggests that carbon is retained upon heating to 1000 °C. The associated DTG curve distinguishes four regions during decomposition. This finding is confirmed using the Lorentz simulation, since a simulated four-peak curve really matched the weight loss rate of the poly[*B*-(methylamino)borazine] as a function of temperature. Each weight loss is associated with two steps which seem to proceed simultaneously.

Weight losses and decomposition rates (Differential Thermogravimetric (DTG) data) have been also monitored during thermal decomposition of BmPS of the type [B(C₂H₄SiCH₃NH)₃]ₙ (C₂H₄ = CH₃CH, CH₂CH₂) by TGA in flowing nitrogen up to 1000 °C (1 °C/min). The result is shown in Fig. 5b. Thermal degradation under nitrogen occurs through a continuous single-step weight loss from 80 °C up to 700 °C providing a black residue. The weight loss after thermolysis at 1000 °C measures *ca.* 46 %. The associated DTG curve distinguishes several decomposition steps. The plotted curve is characterized by one temperature T_{max} = 305 °C at which the decomposition rate is maximum, but the presence of smaller peaks and the broadening and asymmetry of some peaks due to

peak overlapping, suggested a more complicated decomposition process which has been simulated with five peaks using the Lorentz multi-peaks function.

(a)

(b)
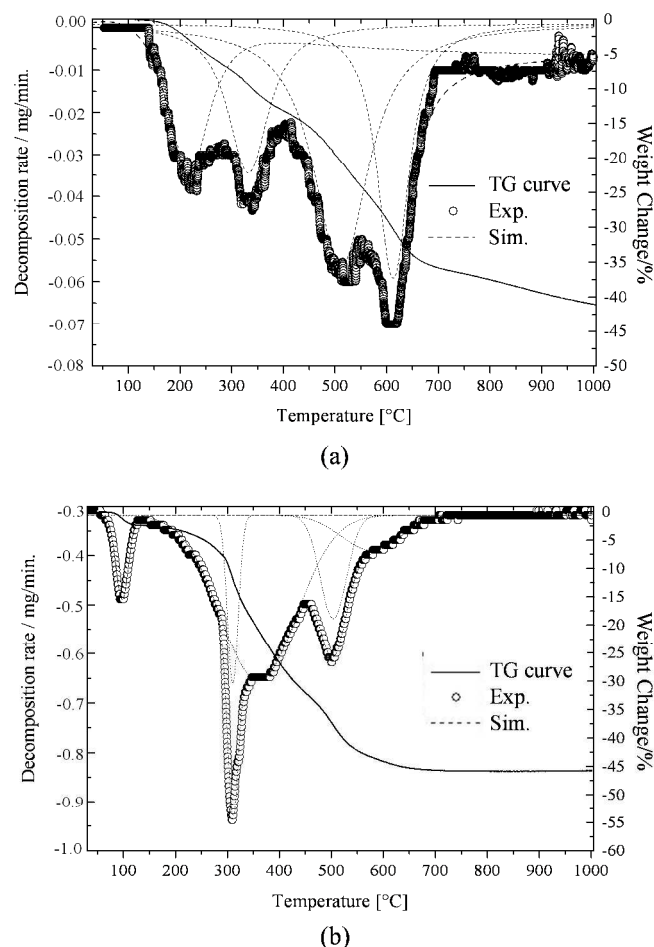
Figure 5. TGA, experimental and simulated DTG curves for poly[*B*-(methylamino)borazine] (a) and BmPS of the type [B(C₂H₄SiCH₃NH)₃]ₙ (C₂H₄ = CH₃CH, CH₂CH₂) (b) in a nitrogen atmosphere. Heating rate: 1 °C/min.

At 1000 °C, **B/C/N**@CMK-3 and **Si/B/C/N**@CMK-3 samples are obtained. Subsequently to the pyrolysis step, the template removal is achieved under ammonia through heat-treatment at 1000 °C with a dwelling time of 5 h. The heating rate is fixed at 5 °C/min. Decomposition starts at 750 °C and continues during the plateau at 1000 °C. A dwelling time of 5 h is required to match the expected weight loss according to the quantity of carbon template used during the polymer impregnation. In fact, this treatment has two objectives: it allows the removing of the template while a part of the residual carbon present in B/C/N and Si/B/C/N samples was removed. This offers the interest to prepare **OMPBN** from poly[*B*-(methylamino)borazine] free of carbon whereas **OMPSi/B/C/N** samples are produced after pyrolysis at 1000 °C with free carbon in a lower content in comparison to conventional polymer-derived Si/B/C/N materials. The samples are generated as micron-sized plate-like powders with an excellent

order after the template removal as shown through the HRTEM images (*See Supporting Information in Fig. SI1*).

The cross-section HRTEM images clearly display a hexagonal (honeycomb-like) arrangement of the mesopores with regular diameters in the mesopore domain. Textural properties of both samples are summarized in Table 1.

Table 1. Textural properties of samples **OMPBN** and **OMPSi/B/C/N**.

Sample	Total Pore Volume (cm³/g)[a]	Mesopore Volume (cm³/g)[b]	BET Surface Area (m²/g)	Average Pore Diameter (nm)
OMPBN	0.73	0.22	1100	4.1
OMPSi/B/C/N	0.78	0.73	544	4.6

[a]*Total Pore Volume at P/Po = 0.95*
[b]*Calculated according to the BJH (adsorption branch between 0.4 < P/Po < 0.95)*

Based on BET experiments and the IUPAC classification of the sorption isotherms[67], the pore size distribution showed a mesopores population centred on 4.1 nm (**OMPBN**) and 4.6 nm (**OMPSi/B/C/N**) whereas the total pore volume was 0.73 cm³/g (**OMPBN**) and 0.78 cm³/g (**OMPSi/B/C/N**). The specific surface area was 1100 m²/g (**OMPBN**) and 544 m²/g (**OMPSi/B/C/N**) (Table 1). The difference in terms of BET surface area between both samples is difficult to explain whereas the ceramic yields of both polymers are similar. This results from the difference in the solubility of the polymers: the poly[*B*-(methylamino)borazine] exhibits a higher solubility in common solvent than the BmPS of the type $[B(C_2H_4SiCH_3NH)_3]_n$ ($C_2H_4 = CH_3CH, CH_2CH_2$). It should be mentioned that the N_2 adsorption-desorption isotherms of **OMPSi/B/C/N** is discussed later together with the N_2 adsorption-desorption isotherms of **HPSi/B/C/N**.

LA-XRD experiments allowed us to calculate a lattice parameter a_{100} of 8.30 nm (**OMPBN**) and 8.01 nm (**OMPSi/B/C/N**) according to the presence of a clear diffraction peak with d = 7.2 nm (2θ = 1.08 °, **OMPBN**) and 6.94 nm (2θ = 1.27 °, **OMPSi/B/C/N**) assigned to the (100) reflection of the 2-D hexagonal lattice (space group *P6mm*) (*See Supporting Information in Fig. SI2*).

C Processing of ordered mesoporous BN and Si/B/C/N powders into monolith-type parts

Powder processing is the preferred method of producing ceramic materials. In the early sixties, Japanese researches designed a process where an applied electric current induced the necessary temperature increase to sinter various powders.[68,69] Several companies produced machines based on this invention according to the significant interest of both the academic and industrial communities. Spark Plasma Sintering (SPS) is one of these processes.

SPS is a pulse current processing that has mainly been used to produce dense ceramic materials.[70] In the process, the pulse direct current used can pass through the graphite die, punch rods and the samples causing the acceleration of the neck

formation between the grains compared to the other sintering techniques. Combined with the rapid heating rates which suppresses grain growth, a fine-grained micro-/nano-structure is obtained. The detailed understanding of the process is still a topic of intense debate but this is not the topic of the present paper. Because of the rapid heating rates, materials processing is complete within short periods of approximately 30 minutes. The possibility to process materials at comparably low temperatures combined with short processing times enables tight control over grain growth, microstructure and densification. SPS can also be used to produce partially sintered materials from different powders. For example, there are reports on the preparation of porous materials using SPS such as zeolithes[71-72], alumina[73], silica[74]. Porous silicon carbide have also been prepared by SPS at 1900-2000 °C from nanosized β-SiC and sintering additives (α-Al_2O_3, Y_2O_3, AlN). Porosities in the range 32-39 % have been measured with no indication of the specific surface area.[75]

Here, we describe how spark plasma sintering (SPS) has been employed to produce mechanically stable, hierarchically meso/macro porous monoliths from **OMPBN** and **OMPSi/B/C/N** samples.[76-77] It should be noted that hierarchically porous materials with well-defined macroscopic shapes (e.g. cylinders) are commonly called monoliths in the scientific literature.

Because of the formation of multiscale porosity is strongly affected by the temperature of sintering which depends on the structure and composition of the considered material to be sintered, it is necessary to distinguish BN and Si/B/C/N materials according to their structural difference.

BN is a crystalline compound located between III and V group elements in the Periodic Table with such a system. It is important to find a compromise which allows obtaining a sufficient crystallinity (to propose the intrinsic properties of BN) without affecting the specific surface area.

Si/B/C/N materials are in general amorphous and exhibit atomically homogenous elemental distributions. The use of amorphous inorganic networks is appeared to be a promising approach to solve or limit the problem of cleavage along the lowly indexed lattice planes in crystalline materials leading to their brittleness. Although Si/B/C/N materials are not in the global thermodynamic equilibrium state, which might be a disadvantage with respect to the desired thermal and/or mechanical durability, they demonstrated high kinetic stability, and thus durability because of an appropriate choice of the element combinations which compose the ceramic network. However, the risk of temperature-induced structural and textural changes, *e.g.* phase transformation of the amorphous Si/B/C/N phase into the thermodynamically phases (Si_3N_4/SiC/B(C)N/C) and pore collapse, typically limit the maximum temperature for this composition.

Based on the dilatometry curves for each system, we decided to fix a SPS temperature of 1600 °C for **OMPBN** samples and a temperature of 800 °C for the Si/B/C/N system (**OMPSi/B/C/N**). These differences in the sintering temperatures proof the strong correlation between the ceramic

composition/structure and the temperature of the process. In addition, SPS experiments have been performed without pressure (**OMPBN**) or under a low compressive stress (16 MPa, **OMPSi/B/C/N**) using a classic heating rate (100 °C.min^{-1}) with the objective to retain a certain level of mesoporosity present in the pristine powders while creating novel forms of porosity using, in particular, the space formed by necking between the grains. Typical examples of the monoliths labelled **HPBN** and **HPSi/B/C/N** are presented in Fig. 6.
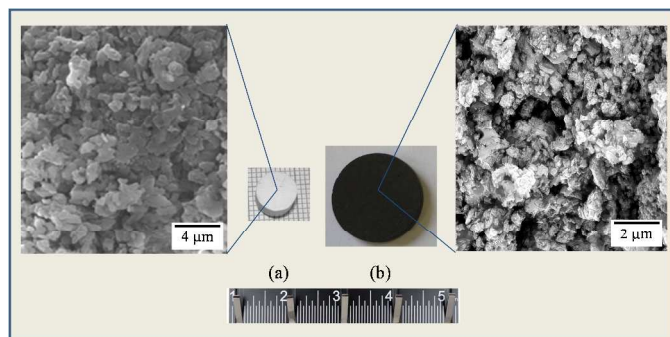
Figure 6. Photographs and corresponding SEM images of the samples **OMPBN** (a) and **OMPSi/B/C/N** (b).

No cracks were found in these monoliths by the naked eye. All monoliths discussed in this paper have an excellent tablet-like appearance and replicated the cylindrical shape of the fabrication die.

The SEM image of the fracture surface for each samples (Fig. 6) showed a microstructure with a grain morphology which differs from that one observed in powders. "Necks" are formed around the area of contact between particles which is the results of a powder sintering by SPS.[78] This is particularly true for BN samples most probably due to the high SPS temperature which has been applied. Furthermore, we clearly observe the presence of voids with different shapes and diameters resulting from the limited densification of powders. It should be mentioned that grain growth does not occur during sintering since XRD patterns of as-obtained monoliths are similar to those of pristine powders (*See Supporting Information in Fig. SI3*).

The mesostructural ordering of the monoliths investigated by LA-XRD measurements confirmed that the mesostructural ordering observed in **OMP** samples is retained in the derived monoliths (**HP**) with a d_{100} value of 8.0 nm (**HPBN**) and 7.29 nm (**HPSi/B/C/N**) and a deduced cell parameter a_{100} of 9.23 nm (**HPBN**) and 8.42 nm (**HPSi/B/C/N**). Samples **HPBN** and **HPSi/B/C/N** are particularly interesting because they demonstrated mesoporosity according to the nitrogen sorption isotherms. As an illustration, we present the BET isotherm of **HPSi/B/C/N** samples (Fig. 7). Analysis of the isotherms demonstrated that the monoliths show IV type-curve typical for mesoporous adsorbents with distinct capillary condensation branches in the relative pressure ranges 0.40 - 1.0. This suggested that the materials retain open/closed mesoporous channels as it has been observed for pristine powders. On the

other hand, the shape of isotherms is asymmetrical with a desorption branch steeper than the adsorption branch at a relative pressure (*P/Po*) from 0.40 to 0.72 indicative of H2 hysteresis loops which are generally found in disordered porous materials or in ordered mesoporous material with 3-D cage-like pores and interconnected pores.[79-80] The absence of large gas adsorption at low relative pressure values reflected the disappearance of micropores which are present in the pristine powders.
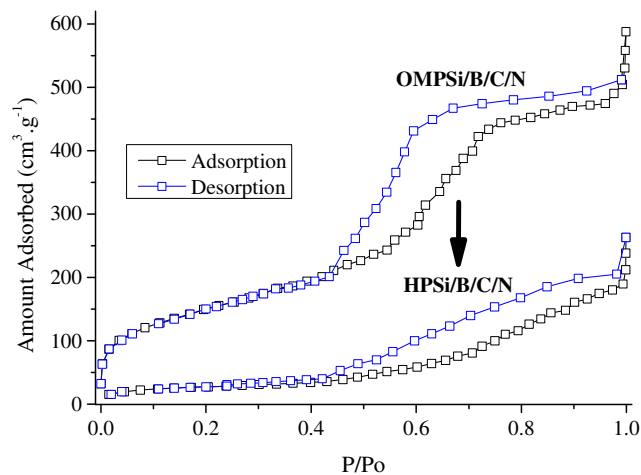
Figure 7. N_2 adsorption-desorption isotherms of samples **HPSi/B/C/N**.

The corresponding textural properties obtained for monoliths are presented in Table 2.

Table 2. Textural properties of samples **HPBN** and **HPSi/B/C/N**.

Sample	Total Pore Volume (cm^3/g)^a	Mesopore Volume (cm^3/g)^b	BET Surface Area (m^2/g)	Average Pore Diameter (nm)
HPBN	0.33	0.20	428	4.3
HPSi/B/C/N	0.35	0.33	154	6.4

^{a}*Total Pore Volume at P/Po = 0.95*
^{b}*Calculated according to the BJH (adsorption branch between 0.4 < P/Po < 0.95)*

Analysis of the isotherms allowed to measure specific BET surface areas ranging of 428 (**HPBN**) to 154 m²/g (**HPSi/B/C/N**) which decreased by more than 2 in comparison to **OMP** samples due to the collapse of the microporosity. The mesopore size was centred at 4.3 nm (**HPBN**) and 6.4 nm (**HPSi/B/C/N**) whereas the total pore volume decreased to 0.20 cm^3/g (**HPBN**) and 0.33 cm^3/g (**HPSi/B/C/N**) which confirmed the compaction of monoliths during SPS experiments.

The presence of mesopores in the monoliths is also confirmed by HRTEM experiments as shown with the **HPBN** sample (Fig. 8). It is difficult to distinguish a periodically ordered mesoporosity in the sample **HPBN** with low resolution TEM. In contrast, HRTEM allowed observing the presence of mesopores which are mostly surrounded by stacked BN layers. They seem to be locally ordered. Based on these observations, it is proven that SPS retains a minimum level of ordered mesoporosity (intragranular porosity) present in samples.
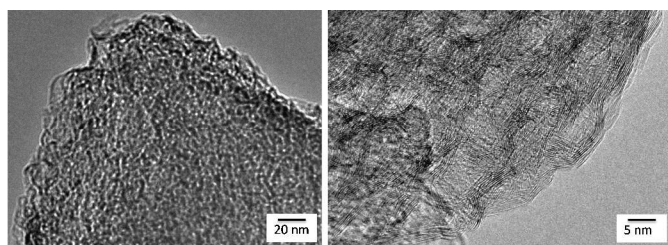
Figure 8. TEM images of the sample **HPBN**.

Table 3 reports the data obtained by helium pycnometry.

Table 3. Data collected by Helium pycnometry of samples **HPBN** and **HPSi/B/C/N**.

Sample	Bulk Density[a]	Helium Density	Macropore Volume (cm³/g)[b]	Porosity (%)
HPBN	0.786	2.18	0.63	64
HPSi/B/C/N	0.676	2.21	0.70	69

[a] Ratio of the mass of the monolith sample and its total volume(three replicate determinations have been achieved for the determination of this property)
[b] Calculated according to $V_{macro} = 1/d_a - 1/d_h - V_{meso}$ (by deliberately omitting microporous volume).

The bulk (from 0.676 to 0.786) and helium (from 2.18 to 2.21) densities of both samples are very close. Therefore, the deduced porosity of samples decreased from 69 % (**HPSi/B/C/N**) to 64 % (**HPBN**) which demonstrated that SPS experiments allowed retaining a very high porosity in the monoliths.

The macropore volume was calculated based on Eq. (1).

$$V_{macropores} = 1/d_B - 1/d_{He} - V_{mesopores} \qquad (1)$$

, where d_B is the bulk density (ratio of the mass of the monolith sample and its total volume which includes particle volume, inter-particle void volume and internal pore volume) and d_{He} is the helium density measured by helium pycnometry.

It should be mentioned that we have neglected the contribution of micropores in Eq. (1) based on BET experiments which highlighted an absence of large gas adsorption at low relative pressure values in monoliths. According to Eq. (1), we calculated a macropore volume which increased from 0.63 cm³/g (**HPBN**) to 0.>70 cm³/g (**HPSi/B/C/N**).

Perspectives

First examples of hierarchically porous Polymer-Derived Ceramic (PDC) monoliths have been prepared by spark plasma sintering (SPS) from an assembly of ordered mesoporous powders displaying *P6mm* hexagonal symmetry without the use of additives. We particularly reviewed the preparation of BN and Si/B/C/N materials. The coupled approach (PDCs route and SPS process) allowed obtaining robust monoliths with high porosity which is related to the use of ordered mesoporous powders as starting materials and to the control and the tailoring of the pore size and the connectivity over a relatively wide range of length scales through the parameters of sintering. Furthermore, the use of SPS inhibited grain growth during sintering leading to materials which retained the intrinsic properties of the pristine powders.

An important aspect of the current research is the extension of the underlying processing method to a wider range of non-oxide materials including binary systems, nanocomposites and solid solutions. To date, the combination of PDCs with controlled porosity and SPS is vastly unexplored. However, because of the versatility of the PDCs route this two-step approach should open the way to a very broad set of monolithic materials in terms of composition, textures, structures and shapes. It can be reasonably anticipated that this will lead to the preparation of a new generation of ceramics for environment and energy technologies as catalysts or supports.

Notes and references

IEM (Institut Europeen des Membranes), UMR 5635 (CNRS-ENSCM-UM2), Universite Montpellier 2, Place E. Bataillon, F- 34095, Montpellier, France; Philippe.Miele@univ-montp2.fr

1   R. T. Paine, C. K. Narula, *Chem. Rev.* 1990, **90**, 73.

2   W.-Q. Han, editor. Anisotropic hexagonal boron nitride nanomaterials: synthesis and applications. 2008: Wiley-VCH Verlag GmbH & Co. KGaA.

3   Y. Kubota, K. Watanabe, O. Tsuda, T. Taniguchi, *Science*, 2007, **317**, 932.

4   K. Watanabe, T. Taniguchi, T. Niiyama, K. Miya, M. Taniguchi, *Nat Photonics.*, 2009, **3**, 591.

5   D. Golberg, Y. Bando, Y. Huang, T. Terao, M. Mitome, C. C. Tang, C. Y. Zhi *ACS Nano.* 2010, **4**, 2979.

6   M. Bechelany, A. Brioude, P. Stadelman, S. Bernard, D. Cornu, P. Miele, *J. Phys. Chem. C*, 2008, **112**, 18325.

7   J. Robertson *Phys Rev B.* 1984, **29**, 2131.

8   S. H. Jhi, Y. K. Kwon, *Phys Rev B.* 2004, **69**, 245407.

9   G. Lian, X. Zhang, S. Zhang, D. Liu, D. Cui, Q. Wang, W *Energ. Environ. Sci.* 2012, **5**, 7072

10   J. Li, J. Lin, X. Xu, X. Zhang, Y. Xue, J. Mi, Z. Mo, Y. Fan, L. Hu, X. Yang, J. Zhang, F. Meng, S. Yuan, C. Tang, *Nanotech.* 2013, **24**, 155603.

11   Q. Sun, Z. Li, D.J. Searles, Y. Chen, G. Lu, A. Du, *J. Am. Chem. Soc.*, 2013, **135**, 8246.

12   W. Lei, D. Portehault, D. Liu, S. Qin, Y. Chen, *Nat. Commun.*, 2013, **4,** 1777.

13   J. Li, X. Xiao, X. Xu, J. Lin, Y. Huang, Y. Xue, P. Jin, J. Zou, *Nature*, 2013, **3**, 3208.

14   (a) Z. Zhou, Y. Hu, H. Wang, Z. Xu, W. Wang, X. Bai, X. Shan, X. Lu, *Nature*, 2013, **3**, 3287; (b) S. Liu, B. Lu, Q. Zhao,

J. Li, T. Gao, Y. Chen, Y. Zhang, Z. Liu, Z. Fan, F. Yang, L. You, D. Yu, *Adv. Mater.*, 2013, **25**, 4549.

15 Z. Zhang, K. Leinenweber, M. Bauer, L. A. J. Garvie, P. F. McMillan, G. H. Wolf, *J. Am. Chem. Soc.*, 2001, **123**, 7788.

16 R. Riedel, G. Mera, R. Hauser, A. Klonczynski, *J. Ceram. Soc. Jpn*, 2006, **114**, 425.

17 P. Colombo, G. Mera, R. Riedel, G.D. Soraru, *J. Am. Ceram. Soc.* 2010, **93**, 1805.

18 X.B. Yan, L. Gottardo, S. Bernard, P. Dibandjo, A. Brioude, H. Moutaabbid, P. Miele, *Chem. Mater.* 2008, **20**, 6325.

19 O. Majoulet, J.G. Alauzun, L. Gottardo, C. Gervais, M.E. Schuster, S. Bernard, P. Miele, *Micro. Meso. Mater.* 2011, **140**, 40.

20 S. Bernard, O. Majoulet, F. Sandra, A. Malchere, P. Miele, *Adv. Engineer. Mater.*, 2013, **15**, 134.

21 R. Riedel, A. Kienzle, W. Dressler, L. Ruwisch, J. Bill, F. Aldinger, *Nature*, 1996, **382**, 796-798.

22 F. Aldinger, M. Weinmann, J. Bill, *Pure Appl. Chem.*, 1998, **70**, 439.

23 M. Weinmann, R. Haug, J. Bill, F. Aldinger, J. Schuhmacher, K. Müller, *J. Organomet. Chem.* 1997, **541**, 345.

24 T. Wideman, E. Cortez, E.E. Remsen, G.A. Zank, P.J. Carrol, L. G. Sneddon, *Chem. Mater.* 1997, **9**, 2218.

25 D. Srivastava, E. N. Duesler, R. T. Paine, *Eur. J. Inorg. Chem.* 1998, **1998**, 855.

26 H. P. Baldus, M. Jansen, D. Sporn, *Science*, 1999, **285,** 699.

27 Weinmann, M.; Schuhmacher, J.; Kummer, H.; Prinz, S.; Peng, J.; Seifert, H. J.; Christ, M.; Müller, K.; Bill J. and Aldinger F. *Chem. Mater.*, 2000, **12**, 623.

28 Z-C Wang, F Aldinger, R. Riedel, *J. Am. Ceram. Soc.*, 2001, **84**, 2179.

29 M. Weinmann, T. W. Kamphowe, J. Schuhmacher, K. Müller, F. Aldinger, *Chem. Mater.*, 2000, **12**, 2112.

30 (*a*) S. Bernard, M. Weinmann, D. Cornu, P. Miele, F. Aldinger *J. Eur Ceram. Soc.* 2005, **25**, 251; (*b*) S. Bernard, M. Weinmann, P. Gerstel, P. Miele, F. Aldinger *J Mater Chem.* 2005, **5**, 289; (*c*) S. Bernard, S. Duperrier, D. Cornu, P. Miele, M. Weinmann, C. Balan, F. Aldinger, *J. Optoelectron. Adv. M.*, 2006, **8**, 648; (*d*) L. Gottardo, S. Bernard, M.-P. Berthet, P. Miele, *Key Engineer. Mater.*, 2008, **368-372**, 926; (*e*) L. Gottardo, S. Bernard, C. Gervais, K. Inzenhofer, G. Motz, M. Weinmann, C. Balan, P. Miele *J. Mater. Chem.* 2012, **22**, 7739; (*f*) L. Gottardo, S. Bernard, C. Gervais, M. Weinmann, P. Miele, *J. Mater. Chem.* 2012, **22**, 17923; (*g*) T. Ouyang, L. Gottardo, S. Bernard, R. Chiriac, C. Balan, P. Miele, *J. Appl. Polym. Sci.*, 2013, **128**, 248.

31 (*a*) "Better Ceramics Through Chemistry III", *MRS Symp. Proc.*, 1988, *121*, 465; (*b*) "Better Ceramics Through Chemistry IV", *MRS Symp. Proc.*, 1994, **346**, 593.

32 P. Sajgalik, *Pure Appl. Chem.*, 2002, **74**, 2137.

33 R. Riedel, From Molecules to Materials-A novel route for the synthesis of advanced ceramics, *Naturwissenschaften*, 1995, **82**, 12-20.

34 P. Miele, S. Bernard, D. Cornu, B. Toury, *Soft. Mater.* 2006, **4**, 249.

35 R. Riedel, E. Ionescu, I.-W. Chen, Modern Trends in Advanced Ceramics in *Ceramics Science and Technology. Vol.1: Structures*. R. Riedel, I-W. Chen, (Eds.) Wiley-VCH, Weinheim, 2008.

36 P. Colombo, G.D. Soraru, R. Riedel, H.J. Kleebe, (Eds). *Polymer Derived Ceramics. From Nano-Structure to Application*. DEStech Publications, Lancaster, PA, 2009.

37 S. Bernard (Ed), Design, Processing and Properties of Ceramic Materials from Preceramic Precursors in *Materials Science and Technologies*, Nova Publishers, 2012.

38 E. Ionescu, Polymer derived Ceramics, in *Ceramics Science and Technology, Vol. 3*. Riedel, R.; Chen, I-W. (Eds.) Wiley-VCH, Weinheim, 2012, pp. 457-500.

39 (*a*) V. Salles, S. Bernard, A. Brioude, D. Cornu, P. Miele, *Nanoscale*, 2010, **2**, 215; (*b*) S. Duperrier, S. Bernard, A. Calin, C. Sigala, R. Chiriac, P. Miele, C. Balan, *Macromolecules* 2007, **40**, 1028.

40 Z. Jiang, L.V. Interrante, *Chem. Mater.*, 1990, **2**, 439.

41 D. Seyferth, G. Mignani, *J. Mater. Sci. Lett.* 1988, **7**, 487.

42 Z. Xie, S. Cao, J. Wang, X. Yan, S. Bernard, P. Miele *Mater. Sci. Eng. A,* 2010, **527**, 7086.

43 E. Ionescu, H.-J. Kleebe, R. Riedel, *Chem. Soc. Rev.* 2012, **41**, 5032.

44 M. Zaheer, T. Schmalz, G. Motz, R. Kempe, *Chem. Soc. Rev.* 2012, **41**, 5102.

45 Y. Shi, Y. Wan, D. Zhao, *Chem. Soc. Rev.*, 2011, **40**, 3854.

46 L. Borchardt, C. Hoffman, M. Oschatz, L. Mammitzsch, U. Petasch, M. Hermann, S. Kaskel, *Chem Soc. Rev.* 2012, **41**, 5053.

47 (a) P. Dibandjo, L. Bois, F. Chassagneux, D. Cornu, J.M. Létoffé, B. Toury, F. Babonneau, P. Miele, *Adv. Mater.* 2005, **17**, 571 ; (b) P. Dibandjo, F. Chassagneux, L. Bois, C. Sigala, P. Miele, *J. Mater. Chem.*, 2005, **15**, 1917 ; (c) P. Dibandjo, L. Bois, F. Chassagneux, P. Miele, *J. Eur. Ceram. Soc.*, 2007, **27**, 313.

48 Y. F. Shi, Y. Meng, D. H. Chen, S. J. Cheng, P. Chen, T. F. Yang, Y. Wan, D. Y. Zhao, *Adv. Funct. Mater.*, 2006, **16**, 561.

49 J. Yan, A.J. Wang, D.P. Kim, *J. Phys. Chem. B* 2006, **110**, 5429.

50 P. Krawiec, S. Kaskel, *J. Solid. State Chem.*, 2006, **179**, 2281.

51 P. Krawiec, D. Geiger, S. Kaskel, *Chem. Comm.* 2006, 2469.

52 J. Yan, A. Wang, D.-P. Kim, *Microp. Mesop. Mater.*, 2007, **100**, 128.

53 Q. D. Nghiem, D. Kim, D.P. Kim *Adv. Mater.* 2007, **19**, 2351.

54 Y. Shi, Y. Wan, Y. Zhai, R. Liu, Y. Meng, B. Tu, D. Zhao, *Chem. Mater.*, 2007, **19**, 1761.

55 S. Shiraishi, A. Kikuchi, M. Sugimoto, M. Yoshikawa, *Chem. Lett.*, 2008, **37**, 574.

56 Y. Shi, Y. Wan, B. Tu, D. Zhao, *J. Phys. Chem. C* 2008, **112**, 112.

57 (*a*) J. G. Alauzun, S. Ungureanu, N. Brun, S. Bernard, P. Miele, R. Backov, C. Sanchez, *J. Mater. Chem.* 2011, **21**, 14025; (*b*) S. Schlienger, J. Alauzun, F. Michaux, L. Vidal, J. Parmentier, C. Gervais, F. Babonneau, S. Bernard, P. Miele Parra, J. B. *Chem. Mater.*, 2012, **24**, 88.

New Journal of Chemistry Accepted Manuscript

58 O. Majoulet, C. Salameh, M.E. Schuster, U.B. Demirci, Y. Sugahara, S. Bernard, P. Miele, *Chem. Mater.*, 2013, **25**, 3957.

59 S. Bernard, P. Miele, *J. Ceram. Sci. technol.*, 2013, **4**, 113.

60 *(a)* V. Salles, S. Bernard, J. Li, A. Brioude, S. Chehaidi, S. Foucaud, P. Miele *Chem. Mater.*, 2009, **21**, 2920; *(b)* J. Li, V. Salles, S. Bernard, C. Gervais, P. Miele, *Chem. Mater.,* 2010, **22**, 2010; *(c)* S. Bernard, V. Salles, J. Li, A. Brioude, M. Bechelany, U. B. Demirci, P. Miele, *J. Mater. Chem.*, 2011, **21**, 8694; *(d)* H. Termoss, B. Toury, S. Payan, A. Brioude, S. Bernard, D. Cornu, S. Vallette, S. Benayoun, P. Miele " *J. Mater. Chem.*, 2009, **19**, 2671; *(e)* M. Bechelany, S. Bernard, A. Brioude, P. Stadelmann, C. Charcosset, K. Fiaty, D. Cornu, P. Miele, *J. Phys. Chem. C,* 2007, **111**, 13378.

61 *(a)* S. Duperrier, R. Chiriac, C. Sigala, C. Gervais, S. Bernard, D. Cornu, P. Miele, *J. Eur. Ceram. Soc.*, 2009, **29**, 851; *(b)* S. Duperrier, C. Gervais, S. Bernard, D. Cornu, F. Babonneau, P. Miele, *J. Mater. Chem.*, 2006, **16**, 3126; *(c)* S. Bernard, K. Fiati, P. Miele, D. Cornu, P. Laurent, *J. Phys. Chem. B*, 2006, **110**, 9048; *(d)* P. Toutois, P. Miele, S. Jacques, D. Cornu, S. Bernard, *J. Am. Ceram. Soc.*, 2006, **89**, 42; *(e)* S. Bernard, F. Chassagneux, M.-P. Berthet, D. Cornu, P. Miele, *J. Am. Ceram. Soc.*, 2005, **88**, 1607; *(f)* S. Duperrier, C. Gervais, S. Bernard, D. Cornu, F. Babonneau, C. Balan, P. Miele, *Macromolecules*, 2007, **40**, 1018.

62 C. Gervais, F. Babonneau, L. Ruwisch, R. Hauser, R. Riedel, *Can. J. Chem.*, 2003, **81**, 1.

63 G. Schumacher, F. Berger, M. Weinmann, J. Bill, F. Aldinger, K. Muller, *Appl. Organometal. Chem.*, 2001, **15**, 809.

64 F. Berger, A. Müller, F. Aldinger, K. Müller, *Z. Anorg. Allg. Chem.* 2005, **631**, 355.

65 D. Zhao, J. Feng, Q. Huo, N. Melosh, G. H. Fredrickson, B. F. Chmelka, G. D. Stucky, *Science* 1998, **279**, 548.

66 R. Ryoo, S. H. Joo, S. Jun, S. *J. Phys. Chem. B* 1999, **103**, 7745.

67 (*a*) IUPAC Recommendations *Pure Appl. Chem.* 1985, **57**, 603; (*b*) IUPAC Recommendations *Pure Appl. Chem.* 1994, **66**, 1739; (*c*) C. G. V.Burgess, D. H. Everett, S. Nuttall, *Pure Appl. Chem.* 1989, **61**, 1845.

68 K. Inoue, *Apparatus for electrically sintering discrete bodies*, United States Patent 3250892, 1966.

69 K. Inoue, *Electric-discharge sintering*, United States Patent 3241956, 1966.

70 Z.J. Shen, Z. Zhao, H. Peng, M. Nygren, *Nature*, 2002, **417**, 266-269.

71 P. O. Vasiliev, A. Ojuva, J. Grins, L. Bergstrom, *J. Europ. Ceram. Soc.*, 2010, **30**, 2977.

72 P. Vasiliev, F. Akhtar, J. Grins, J. Mouzon, C. Andersson, J. Hedlund, L. Bergstrom, *ACS Appl. Mater. Inter.*, 2010, **2**, 732.

73 D. Chakravarty, H. Ramesh, T. N. Rao, *J. Europ. Ceram. Soc.*, 2009, **29**, 1361.

74 P. O. Vasiliev, Z. J. Shen, R. P. Hodgkins, L. Bergstrom, *Chem. Mater.*, 2006, **18**, 4933.

75 M. Hotta, H. Kita, H. Matsuura, N. Enomoto, J. Hojo, *J. Ceram. Soc. Jp*, 2012, **120**, 243.

76 P. Dibandjo L. Bois, C. Estournes, B. Durand, P. Miele *Micro. Meso. Mater.* 2008, **111**, 643.

77 O. Majoulet, M. C. Bechelany, F. Sandra, G. Bonnefont, G. Fantozzi, L. Joly-Pottuz, A. Malchere, S. Bernard, P. Miele *J. Mater. Chem. A*, 2013, **1**, 10991.

78 M. Tokita, *J. Powder Technol. Japan,* 1993, **30**, 790.

79 A. Grosman, C. Ortega, *Langmuir*, 2005, **21**, 10515.

80 J. R. Matos, M. Kruk, L.P. Mercuri, M. Jaroniec, L. Zhao, T. Kamiyama, O. Terasaki, T. J. Pinnavaia, Y. Liu, *J. Am. Chem. Soc.* 2003, **125**, 821.

New Journal of Chemistry Accepted Manuscript